Imaging Spectrum of Typical and Atypical Adenomyosis

Alice Brandão, MD • Brunna C. Oliveira, MD, MSc • Ingrid A. G. Ferreira, MD • Luciana G. Matteoni-Athayde, MD • Lucas R. Torres, MD
Luciana Belém, MD, MSc • Izabela P. Franco, MD • Akram M. Shaaban, MBBCh • Douglas Rogers, MD • Luciana P. Chamié, MD, PhD

Author affiliations, funding, and conflicts of interest are listed at the end of this article.
A.B. and B.C.O. contributed equally to this work.

Adenomyosis, characterized by heterotopic endometrial tissue within the myometrium, is a common yet poorly understood condition affecting patients of childbearing age. Although typical features of adenomyosis are extensively discussed in the literature, there is no consensus on its imaging classification. The Morphological Uterus Sonographic Assessment (MUSA) consensus statement is a valuable tool for identifying and describing typical adenomyosis imaging features at US. However, for MRI, there is still no standardized consensus for descriptors and subtypes. The diverse atypical manifestations of adenomyosis are a diagnostic challenge. Familiarity with these manifestations is essential for accurate diagnosis, avoiding misdiagnosis, and ensuring optimal clinical management. The authors examine the imaging appearances of typical and atypical adenomyosis at US and MRI, encompassing focal adenomyosis, diffuse adenomyosis, adenomyomas (solid and cystic types), polypoid adenomyomas, adenomyosis during pregnancy, and malignant transformation. The discussion includes clinical, surgical, and pathologic aspects in the differential diagnosis, with consideration of uterine contractions, deep endometriosis with myometrial infiltration, leiomyomas, and accessory cavitated uterine masses. Practical tips are provided to assist radiologists in distinguishing adenomyosis from other conditions.

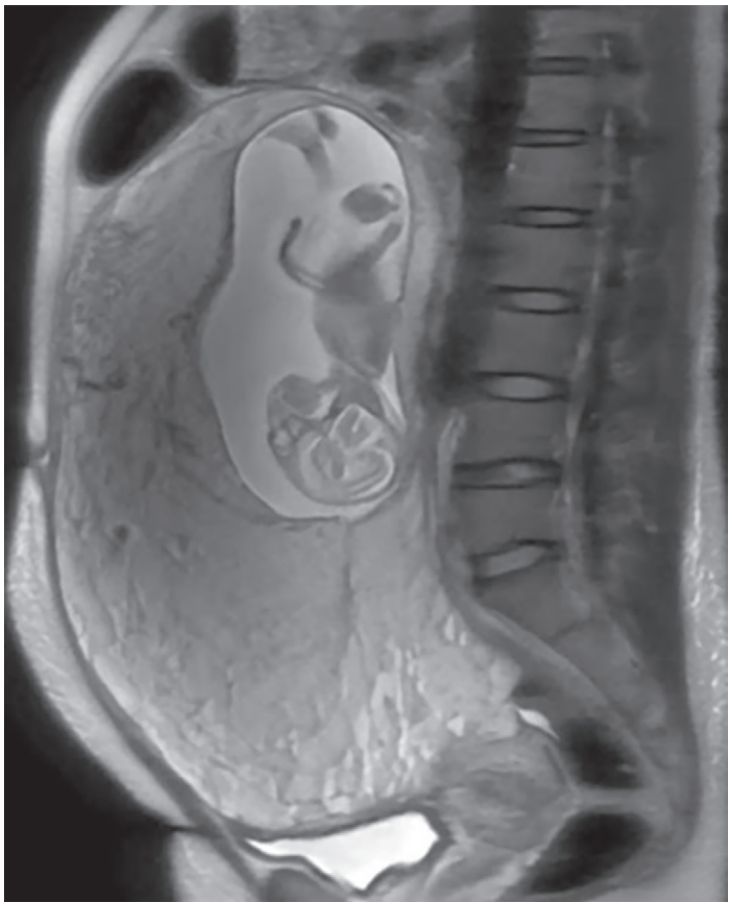

Introduction

Adenomyosis is a benign condition characterized by the presence of heterotopic endometrial tissue, including glands and dense stroma, within the myometrium. This leads to inflammation, neoangiogenesis, fibrosis, and a distortion of the muscular architecture (1). It predominantly affects women during their reproductive years. Determining the prevalence of adenomyosis is challenging, with estimates varying widely from 5% to 70% of reproductive-age women. This variability is partly attributed to the fact that hysterectomy, and thus histologic analysis, the key method for diagnosing adenomyosis, is performed in a specific subset of patients, introducing a selection bias that complicates accurate assessment of prevalence (2).

The pathogenesis of adenomyosis remains poorly understood, and two main theories are broadly accepted. The first theory involves the progression of the disease through invagination of the basal endometrium into the myometrium and is supported by pathologic findings of an indistinct lower boundary between the endometrium and the underlying inner myometrium (3–6). The second theory suggests that intramyometrial embryonic pluripotent müllerian remnants undergo cellular differentiation, leading to adenomyotic islands, which could explain the development of adenomas distant from the junctional zone (JZ) (3,4).

Adenomyosis is linked to diverse risk factors that vary among patients of different age groups and reproductive histories. Studies (7,8) have shown a direct association between adenomyosis and factors such as parity, miscarriages, and uterine surgical procedures such as dilatation and curettage or induced abortion. However, the relationship between adenomyosis and prior cesarean delivery remains a subject of debate, with conflicting results reported in studies (9,10).

Supplemental Material TestYour Knowledge CME

RadioGraphics 2025; 45(5):e240152
https://doi.org/10.1148/rg.240152

Content Codes: MR, OB, US

Abbreviations: ACUM = accessory cavitated uterine mass, JZ = junctional zone, MUSA = Morphologic Uterus Sonographic Assessment

TEACHING POINTS

- Adenomyosis is a benign condition characterized by the presence of heterotopic endometrial tissue, including glands and dense stroma, within the myometrium. This leads to inflammation, neoangiogenesis, fibrosis, and a distortion of the muscular architecture. It predominantly affects women during their reproductive years.
- The typical imaging features of adenomyosis are focal or diffuse thickening of the JZ with intramyometrial cysts. Atypical cases occur less frequently and pose a challenging differential diagnosis with other benign and malignant uterine lesions.
- Although a universally accepted classification system is lacking, the uncommon manifestations of adenomyosis include adenomyomas (solid and cystic), polypoid adenomyomas, adenomyosis during pregnancy, and malignant transformation of adenomyosis.
- Cystic adenomyomas typically exhibit ill-defined margins, lack an internal epithelial lining, and can occur anywhere in the uterus, although they are commonly located near the JZ.
- No definitive endovaginal US or MRI findings indicate malignant transformation. Diagnosis often relies on comparing current imaging studies with previous examinations and applying the following criteria: *(a)* suspicious myometrial location, *(b)* origin from adenomyosis, *(c)* absence of invasion from another source, *(d)* presence of adenomyotic tissue supporting the diagnosis, and *(e)* adenomyotic changes in the surrounding myometrium.

Symptoms of adenomyosis including hypermenorrhea, dysmenorrhea, and chronic pelvic pain (1) typically occur in approximately two-thirds of cases, although they may not correlate with the severity of the disease. In addition, adenomyosis is frequently detected in women facing fertility challenges linked to disrupted myometrial structure and contractility and altered endometrial function (11), affecting pregnancy outcomes, with lower success rates of assisted reproduction treatments and higher miscarriage rates (12). Diffuse forms of adenomyosis appear to have a more pronounced negative effect than focal forms on outcomes of assisted reproductive treatments, emphasizing the need for standardized classification (13). The standard of care for diagnosis of adenomyosis is histologic examination after hysterectomy. However, noninvasive imaging techniques such as US and MRI are emerging as viable diagnostic alternatives (14).

The typical imaging features of adenomyosis are focal or diffuse thickening of the JZ with intramyometrial cysts (15). Atypical cases occur less frequently and pose a challenging differential diagnosis with other benign and malignant uterine lesions. Although there is no consensus on its classification, atypical adenomyosis is usually diagnosed according to variations in tissue composition (ie, solid or cystic) and morphology (ie, nodular or polypoid) (15). Sometimes hormonal changes related to pregnancy or clinical treatments may also induce variations in the composition of adenomyotic tissue, leading to unusual imaging findings (15).

Difficulties in defining its pathogenesis and the lack of a universal classification system have contributed to underdiagnosis and suboptimal clinical management of adenomyosis. Therefore, health care providers should strive to improve their understanding of the diagnosis of adenomyosis, including that of its atypical forms.

The aim of this article is to provide a comprehensive review of usual and unusual manifestations of adenomyosis, including focal adenomyosis, diffuse adenomyosis, adenomyomas (solid and cystic types), polypoid adenomyosis, adenomyosis during pregnancy, and malignant transformation of adenomyosis, comprising their clinical, imaging, surgical, and pathologic aspects. Finally, the main conditions to consider in the differential diagnosis are thoroughly discussed.

Overview of Imaging-based Diagnosis of Adenomyosis

The transition from surgical histologic diagnosis to clinical management in adenomyosis is marked by substantial advancement in imaging-based diagnostics using noninvasive and highly accurate modalities such as endovaginal US and MRI.

The heterotopic endometrium appears as hyperechogenic islands or echogenic subendometrial lines and buds at endovaginal US and as subendometrial hyperintense linear streaks at T2-weighted MRI, while the smooth muscle hyperplasia and hypertrophy is responsible for the ill-defined areas of hypoechogenicity at endovaginal US or low signal intensity at T2-weighted MRI (16). Myometrial cysts characterized by anechoic foci or areas at endovaginal US or by hyperintense foci at T2-weighted MRI are the result of cyclic proliferation and secretion of hormones by the heterotopic endometrial glands and are considered the most reliable sign of adenomyosis (Fig 1). Frequently, these cysts may be filled with hemorrhagic content, appearing as thick hypoechoic fluid at endovaginal US and high signal intensity at T1-weighted MRI (16).

Endovaginal US

Endovaginal US is the first-line diagnostic tool for adenomyosis, with mean sensitivity of 72%, specificity of 81%, and an area under the receiver operating characteristic curve of 0.85 (17,18).

Since 2019, the international Morphological Uterus Sonographic Assessment (MUSA) group has been addressing gaps in US diagnosis of adenomyosis by publishing consensus documents aimed at establishing standardized terminology and classification and reporting systems to describe the morphologic variations and the extent of typical adenomyosis in both two-dimensional and three-dimensional US examinations (19,20). Three-dimensional US is preferred over two-dimensional US, when feasible, due to its enhanced diagnostic accuracy and its ability to allow more-detailed visualization of subtle changes in the JZ, particularly in the cornual region (19,21).

MUSA consensus features are divided into direct and indirect US signs of adenomyosis. Direct features are related to the presence of ectopic endometrial tissue in the myometrium, including myometrial cysts, hyperechogenic islands, and

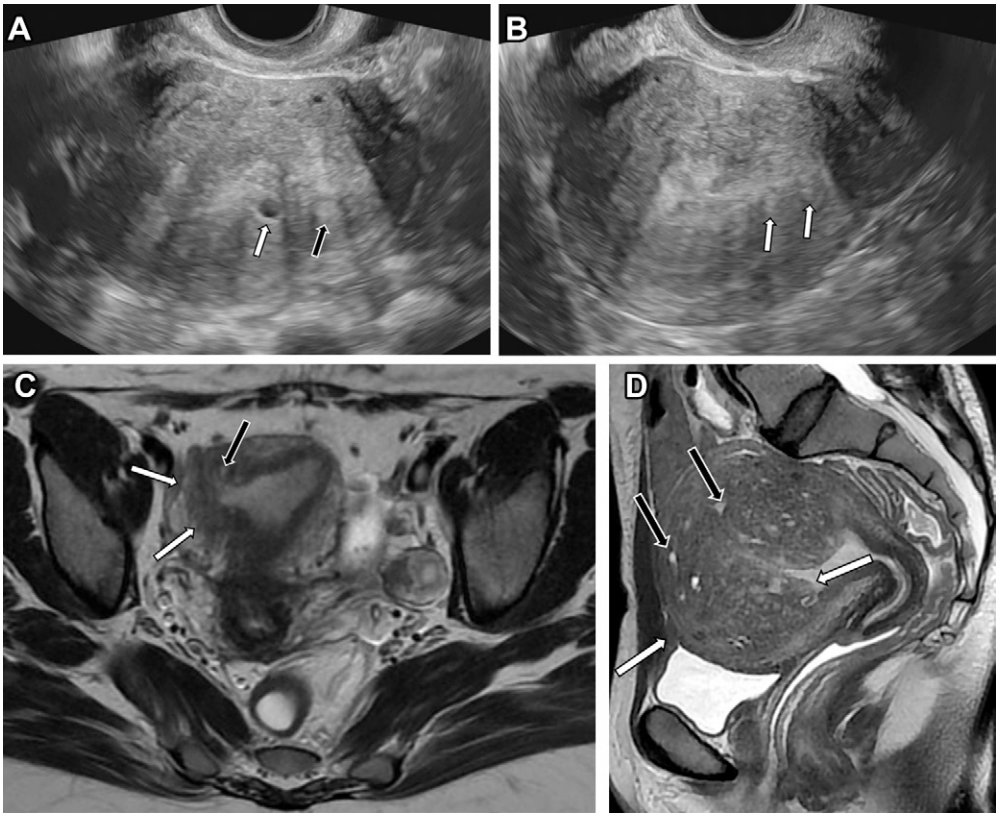

Figure 1. Endovaginal US and MRI features of typical adenomyosis in different patients who are in the menacme. **(A)** Transverse US image shows a myometrial cyst (white arrow) and a hyperechoic island (black arrow). Notice the fan-shaped shadowing. **(B)** Longitudinal US image shows echogenic lines (arrows). **(C)** Axial T2-weighted MR image shows a focal thickening of the JZ (white arrows), with embedded high-signal-intensity foci corresponding to ectopic glands (black arrow). **(D)** Sagittal T2-weighted MR image shows a diffusely enlarged uterus with thickening of the JZ (white arrows) and low signal intensity of the myometrium, with innumerable hyperintense foci (black arrows) scattered in the lesion..

Table 1. Patient Preparation for MRI Assessment of Adenomyosis

Preparation Component	Timing	Purpose
Fasting	4–6 h before examination	Reduces fecal content and, consequently, motion artifacts
Antiperistaltic agent	Administered right before starting the examination, after the patient is positioned	Reduces motion artifacts induced by uterine and bowel peristalsis, improving evaluation of the pelvic organs
Moderate urinary bladder filling	Patient instructed to not urinate starting 1 h before the examination	Prompts visualization of the ureters Avoids detrusor contractions generated by an overfilled bladder

echogenic subendometrial lines and buds. Indirect features result from secondary changes in the myometrium and, therefore, are not conclusive for the diagnosis of adenomyosis in the absence of direct features. The main indirect features are a globular uterus, asymmetric thickening of the myometrial walls, fan-shaped shadowing, translesional vascularity, and irregularity and interruption of the JZ (19,20).

Emerging US technologies such as sonohysterography may provide additional imaging features (5). The infusion of saline solution or microbubble contrast material into the uterine cavity may show continuity between the endometrial cavity and the subendometrial cystic spaces, appearing as flame-shaped or "lollipop" diverticula, an imaging finding also commonly seen in patients affected by adenomyosis who are undergoing hysterosalpingography (5). However, because this additional finding is not crucial for diagnosis, the uterine cavity should only be distended in patients with concurrent uterine conditions (eg, for assessment of adhesions, endometrial polyps, or submucosal leiomyomas).

Magnetic Resonance Imaging

MRI also demonstrates high accuracy in the diagnosis of adenomyosis, with mean sensitivity of 77%, specificity of 89%, and an area under the receiver operating characteristic curve of 0.93 (17). However, due to its lower availability and higher cost compared with those of US, it is sometimes recommended as a problem-solving tool to distinguish equivocal cases or atypical forms. Tables 1 and 2 provide the recommended patient preparation and MRI sequences based on the 2017 European Society of Urogenital Radiology and 2020 Society of Abdominal Radiology guidelines, both developed for the evaluation of endometriotic disease (22–24).

Given the frequent co-occurrence of adenomyosis with other gynecologic conditions such as endometriosis, which is present in approximately 22.3% of patients (25), a more comprehensive approach to pelvic evaluation is often warranted. This may include specialized measures such as bowel preparation and vaginal distention with gel to improve visualization of the bowel and vaginal endometriotic nodules. Although it

Table 2. Recommendations for MRI Assessment of Adenomyosis

Sequence	Planes	Parameters	Importance
T2-weighted fast spin-echo (ie, turbo spin-echo) sequence	Axial Coronal* Sagittal†	Field of view (mm), 260 × 260 Matrix, 320 × 256 Section thickness (mm), 4	Uterine zonal anatomy of the endometrium and JZ Highlights tiny cysts into myometrial lesions or in the JZ Differential diagnosis
T1-weighted fast spin-echo or gradient-recalled-echo sequence	Axial‡	Field of view (mm), 320 × 280 Matrix, 192 × 256 Section thickness (mm), 4	T1-hyperintense hemorrhagic foci
T1-weighted fast spin-echo or gradient-recalled-echo fat-suppressed MRI sequence	Axial Sagittal§	Field of view (mm), 320 × 280 Matrix, 192 × 256 Section thickness (mm), 2–4	T1-hyperintense hemorrhagic foci
Diffusion-weighted MRI	Axial	*b* = 0, 800, 1000, 1200	Evaluation of uterine or adnexal suspicious lesions

Note.—Recommendations also include the use of a 1.5-T or 3-T magnet and a pelvic phased-array coil, with the patient in a supine position, feet first.
* If possible, include volumetric (three-dimensional) coronal plane acquisition.
† An additional T2-weighted fast spin-echo sequence can be performed at the end of the examination to differentiate adenomyosis from transient uterine contractions.
‡ If possible, include volumetric acquisition.
§ If possible, include volumetric acquisition in at least one plane.

does not aid in the diagnosis of typical adenomyosis (24), gadolinium-based contrast material should be administered to characterize atypical features (26) and assist in distinguishing uncommon adenomyosis findings from conditions such as leiomyomas and endometrial polyps.

Typical MRI findings of adenomyosis are similar to those at endovaginal US, and direct (diagnosis-specific) and indirect (inconclusive in isolation) criteria have been defined. The direct criteria include the presence of myometrial cysts, intramyometrial hemorrhagic components, and subendometrial hyperintense linear streaks. The indirect criteria include JZ thickness greater than 12 mm, a maximum JZ thickness to total myometrial thickness ratio greater than 40% (measured at the same point), a maximum to minimum difference in JZ thickness in the anterior and posterior uterine walls greater than 5 mm, a large and smooth uterus, uterine wall asymmetry, and a poorly delimited mass with low signal intensity on T2-weighted MR images (27).

Assessment of JZ

The JZ is a distinct region of myometrium adjacent to the endometrium characterized by a subendometrial halo of low signal intensity at T2-weighted MRI and hypoechoic tissue beyond the endometrial basal layer at US. Evaluating the JZ requires examining multiple orthogonal planes at different time points to distinguish adenomyosis from potential myometrial contractions. MRI is more effective for this assessment due to clearer visualization, although challenges may arise in the early proliferative phase or under hormonal suppression (4,5).

In the context of diagnosing adenomyosis, the importance of JZ thickness (typically averaging 5–12 mm) has evolved over time. Tellem et al (28) identified a JZ thickness of 12 mm or greater as indicative of adenomyosis, predominantly in postmenopausal women. Subsequent research focusing on premenopausal women has challenged this established cutoff measurement. Current evidence derived from MRI–pathologic results correlation studies indicates that irregularities in the JZ or the presence of myometrial cysts may serve as more specific markers for diagnosis of adenomyosis.

Assessment of Severity of Adenomyosis

Evaluation of adenomyosis should encompass all uterine layers including *(a)* the inner layer (JZ), *(b)* the middle layer (between the vascular arcade and the JZ), and *(c)* the outer (subserosal) layer. The involvement of these layers may vary according to the severity of adenomyosis and can influence clinical symptoms (19).

Various histologic and imaging severity classification systems have been proposed, yet international consensus remains elusive. Van den Bosch et al (19) suggest that evaluating the extent of adenomyosis should involve subjective assessment of the proportion of the uterine corpus affected as mild (<25% affected, affecting the JZ), moderate (25%–50% affected), or severe (>50% affected). When lesions are present in multiple locations, the combined volume should be estimated.

However, distinguishing between the JZ and the myometrium can be challenging, particularly with endovaginal US. Therefore, based on our experience, the extent of nonnodular focal or diffuse adenomyosis is most reliably assessed subjectively using endovaginal US or MRI by estimating whether more or less than 50% of the myometrial wall thickness is affected. This approach minimizes errors in interpretation and enhances communication with clinicians.

Typical Adenomyosis

Classification and Characterization

Typical adenomyosis mainly includes the focal or diffuse patterns of the disease. Although some authors classify adenomyomas as a typical form of adenomyosis, this review

Table 3: Typical and Atypical Adenomyosis Imaging Characteristics

Type of Adenomyosis	Imaging Characteristics
Typical adenomyosis	
Focal adenomyosis	Localized signs of adenomyosis with or without JZ bulging, with 25% or more of the circumference of the lesion surrounded by normal myometrium
Superficial adenomyosis	Disseminated signs of adenomyosis without JZ thickening
Diffuse adenomyosis	Disseminated signs of adenomyosis throughout a thickened JZ, with less than 25% of the circumference of the lesion surrounded by normal myometrium
Atypical adenomyosis	
Adenomyoma	Grossly circumscribed adenomyotic mass with less clear borders and mainly solid characteristics, which may manifest as small cystic or hemorrhagic foci
Cystic adenomyoma	Adenomyotic mass with a single or a few large cystic cavities within it
Polypoid adenomyoma	Circumscribed endometrial polypoid mass with heterogeneous imaging appearances, ranging from solid to purely cystic polypoid lesions, in the lower uterine cavity
Adenomyosis during pregnancy	May manifest atypically compared with on previous examinations, showing features such as wall thickening and an increase in the number and size of myometrial cysts
Adenomyosis malignant transformation	Ill-defined isointense or hyperintense lesion on T2-weighted MR images The presence of diffusion restriction increases suspicion

addresses them as an atypical form due to their lower prevalence and occasionally challenging appearance, particularly the cystic type.

The classification of adenomyosis as either focal or diffuse should be determined by estimating the relative proportions of the lesion to the surrounding normal myometrium on a sagittal section image through the uterus, where the lesion is most prominent. *Focal adenomyosis* corresponds to localized signs of adenomyosis with or without JZ bulging, with greater than 25% of the circumference of the lesion surrounded by normal myometrium (19). These may be single or multiple signs. Conversely, *diffuse adenomyosis* is characterized by the presence of disseminated signs of adenomyosis throughout the JZ, which may manifest as symmetric or asymmetric thickening. When there is no JZ thickening, it may also be referred to as superficial adenomyosis (21).

Adenomyosis should be further characterized by its location in the uterine walls (anterior, posterior, lateral left, lateral right, or fundal) and by the presence of intramyometrial cysts, which are considered measurable if their largest diameter exceeds 2 mm. Table 3 summarizes typical and atypical cases of adenomyosis.

Differential Diagnosis

Transient Myometrial Contractions.—Transient myometrial contractions are important to consider in the differential diagnosis of typical and atypical adenomyosis such as adenomyomas. They appear as focal or diffuse sporadic bulging of the myometrium into the uterine cavity, leading to uterine wall asymmetry and slight heterogeneity, which may persist for a few minutes. They appear as hypointense ill-defined bands or nodules perpendicular to the JZ or as focal thickening of the JZ at T2-weighted MRI.

Endometrial displacement or asymmetry helps in distinguishing uterine contractions (in which it is more pronounced) from adenomyomas. However, the key distinguishing feature of uterine contractions is their transient nature. Assessing the uterine myometrium at different time points can help to determine whether the alteration has resolved (Fig 2) (21,26,29).

Deep Endometriosis with Myometrial Infiltration.—Adenomyosis and deep endometriosis may coexist, sharing clinical symptoms such as chronic pelvic pain and dysmenorrhea and having similar histologic and imaging features (30). However, they have a different pathogenesis, epidemiologic characteristics, and clinical implications.

Deep endometriosis often appears as nodules or plaque-like lesions predominantly affecting pelvic ligaments and subperitoneal spaces, often accompanied by adhesions. In severe cases, it can invade the anterior or posterior subserosal myometrium and the middle uterine layer with an outside-in pattern and does not involve the JZ (31). At MRI, myometrial infiltration of deep endometriosis is characterized by an ill-defined mass with low signal intensity at T2-weighted MRI, frequently containing small cystic foci that resemble adenomyosis (Figs 3, S1).

Myometrial infiltration of deep endometriosis is a marker for severe disease, with a high prevalence of associated visceral involvement, frozen pelvis, and low ovarian reserve. These patients tend to experience prolonged painful symptoms and infertility and are likely to have undergone surgery for deep endometriosis in the past. It is technically difficult to resect and requires long surgical times. The complete removal of these lesions may cause a thinning of the uterine wall, which increases the risk of uterine rupture during pregnancy (32).

Atypical Adenomyosis

Although the majority of patients have adenomyosis with typical manifestations, some patients have imaging findings that make diagnosis challenging. Accurate interpretation of the various patterns of adenomyosis requires strong clinical correlation with the patient's hormonal status including

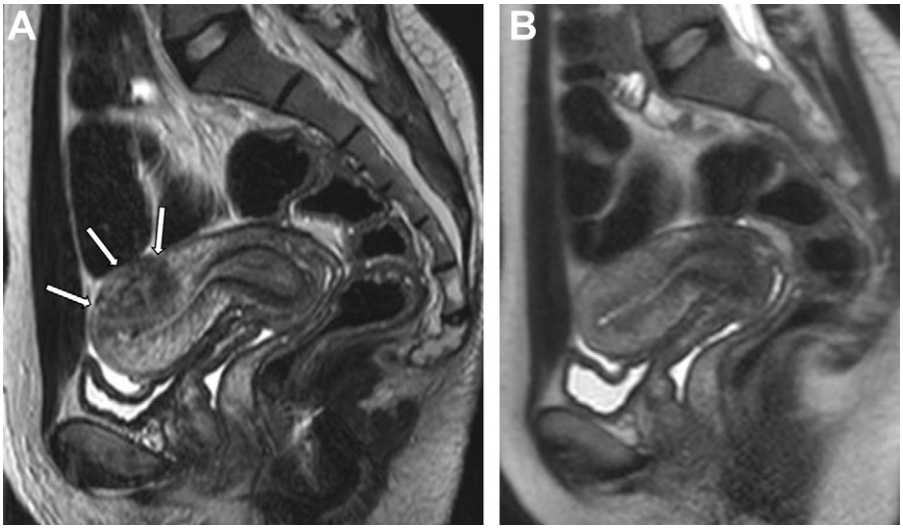

Figure 2. Physiologic transient myometrial contractions simulating adenomyosis in a 26-year-old woman. Sagittal T2-weighted MR images acquired a few minutes apart show a focal area of low signal intensity perpendicular to the JZ on the posterior uterine wall (arrows in **A**) that vanishes after a few minutes **(B)**.

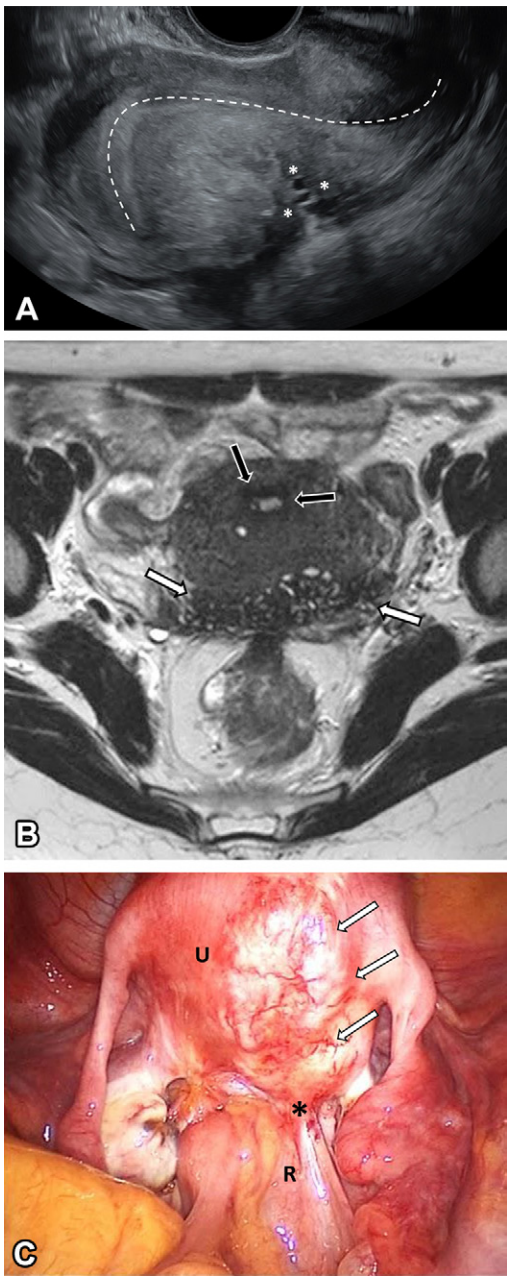

Figure 3. Deeply infiltrative endometriosis in two different women of reproductive age, both with severe dysmenorrhea. **(A)** Longitudinal US image shows a hypoechoic plaque lesion in the posterior uterine serosa, with small cystic areas infiltrating the myometrium (∗) and causing uterine retractile retroflexion (dashed line). **(B)** Axial T2-weighted MR image shows a hypointense lesion in the posterior surface of the uterus, with multiple small hyperintense foci corresponding to endometrial glands (white arrows). The JZ appears normal (black arrows). **(C)** Laparoscopic view shows obliteration of the pouch of Douglas (∗) with the rectum *(R)* tethered to the lesion (arrows) in the posterior aspect of the uterus *(U)*. (Courtesy of Ricardo M. A. Pereira, MD.)

contraceptive use, hormonal stimulation, and pregnancy status (15). Although a universally accepted classification system is lacking, the uncommon manifestations of adenomyosis include adenomyomas (solid and cystic), polypoid adenomyomas, adenomyosis during pregnancy, and malignant transformation of adenomyosis.

Adenomyoma

Adenomyomas are a type of focal adenomyosis, defined as nodular ill-defined lesions surrounded by hypertrophic myometrium. They can manifest as predominantly solid lesions (adenomyomas) or with large cystic components, thereby characterizing them as cystic adenomyomas (21). According to their position, they can be classified as intramural (enclosed in the myometrial wall), submucosal (protruding into the uterine cavity), or subserosal (in the subserosal area of the myometrium, sometimes altering the uterine contour).

Adenomyomas appear at endovaginal US as isoechoic or hypoechoic nodular lesions with poorly defined margins that do not displace the usual myometrial vascular structures. At MRI, they are characterized as nodular lesions that are hypointense on T2-weighted MR images, sometimes showing small intralesional cystic (ie, T2-hyperintense) or hemorrhagic (ie, T1-hyperintense) foci. These lesions persist throughout the examination, and this is a key distinguishing feature from uterine contractions. (Figs 4, 5).

The internal cystic or hemorrhagic contents in adenomyomas may exhibit variability throughout the menstrual cycle.

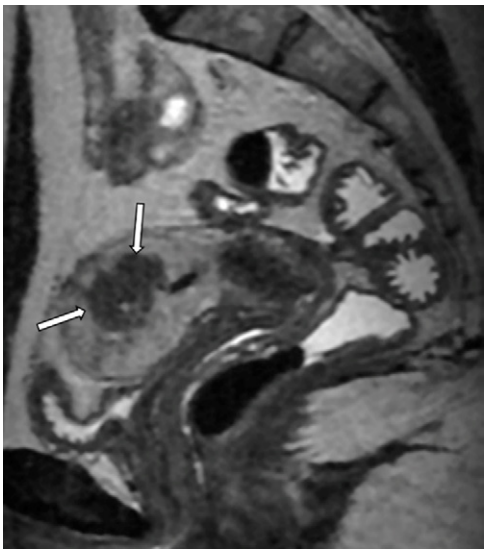

Figure 4. Adenomyoma in a 34-year-old woman with menorrhagia. Sagittal T2-weighted MR image shows a hypointense intramyometrial nodule in the posterior uterine wall, with partially defined margins, minimal mass effect, and small internal hyperintense foci (arrows).

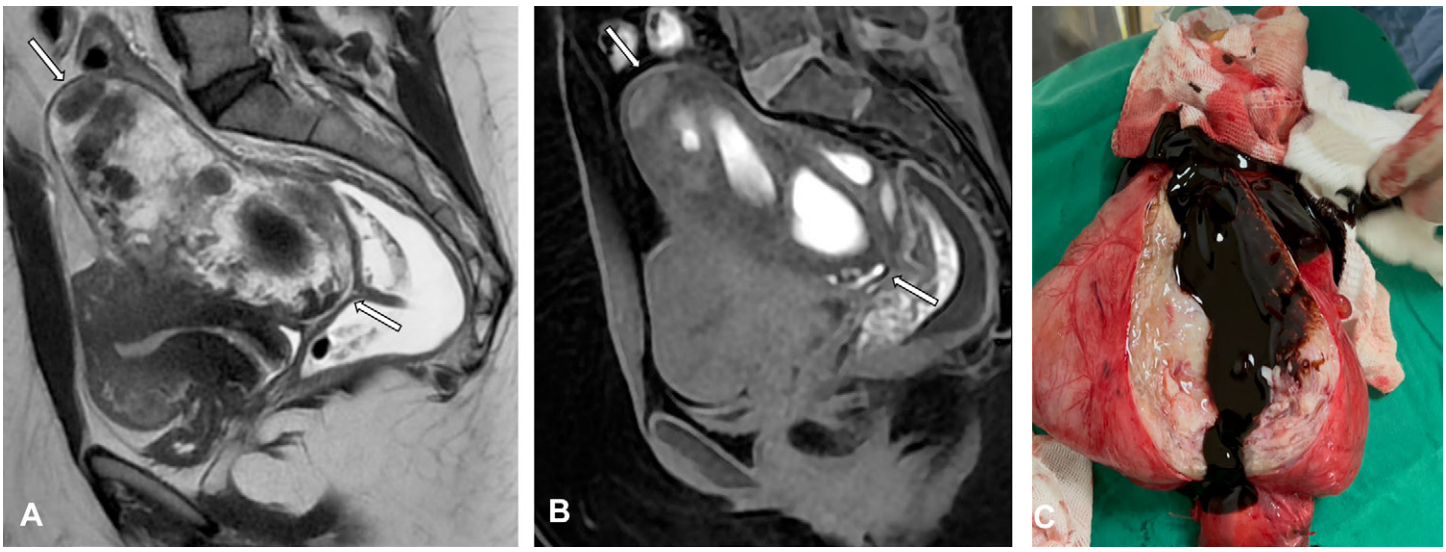

Figure 5. Subserosal adenomyoma in a 36-year-old woman with heavy menstrual cramps since adolescence that worsened in the last year. **(A)** Sagittal T2-weighted MR image shows a subserosal mass (arrows) in the posterior uterine wall, with heterogeneous signal intensity. **(B)** Sagittal T1-weighted MR image with fat saturation shows the mass (arrows) with areas of high signal intensity, indicating hemorrhagic content. **(C)** Photograph of gross specimen shows that it contains a large amount of chocolate-colored fluid. (Case courtesy of Marcello Lemgruber, MD.)

These changes become more apparent during the late secretory phase preceding menstruation; therefore, imaging during this phase may enhance visibility and potentially reduce the likelihood of misdiagnosis. In addition, these contents may vary with the administration of hormonal therapies (24).

Cystic Adenomyoma

Cystic adenomyomas are characterized by a single or a few large cystic hemorrhagic cavities with high signal intensity at T1-weighted MRI (hemorrhagic content), sometimes with a fluid–fluid level, and are surrounded by a thick and irregular wall that shows low signal intensity at T2-weighted MRI (Figs 6, 7) (21). Cystic adenomyomas typically exhibit ill-defined margins, lack an internal epithelial lining, and can occur anywhere in the uterus, although they are commonly located near the JZ.

In adult patients, especially during pregnancy, the main condition to consider in the differential diagnosis is leiomyoma with hemorrhagic degeneration. Cystic adenomyoma should be carefully distinguished from an accessory cavitated uterine mass (ACUM), which was previously referred to as *juvenile cystic adenomyoma* in young women and is located below the uterine insertion of the round ligament (21). Figure 8 compiles valuable information for distinguishing a cystic adenomyoma from a leiomyoma with cystic degeneration, an ACUM, and a unicornuate uterus with a functional uterine remnant (Fig S2). The differential diagnosis for adenomyomas includes conditions such as leiomyomas, transient myometrial contractions, ACUMs, intramural pregnancy, and adenomatoid tumors.

Differential Diagnosis

***Leiomyomas.*—**Leiomyoma, a benign smooth-muscle tumor, is a primary consideration in the differential diagnosis of adenomyoma. The main distinctions between adenomyomas and

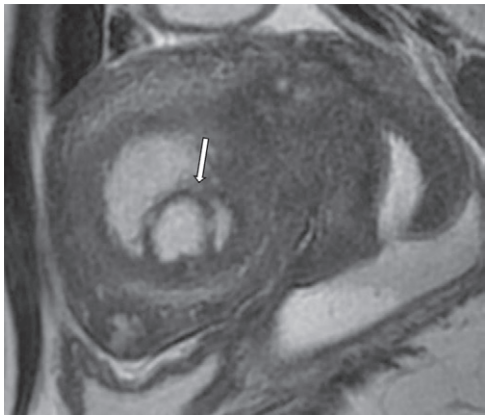

Figure 6. Submucosal cystic adenomyoma in a 45-year-old woman with infertility. Sagittal T2-weighted MR image show a round heterogeneous cystic lesion (arrow) distorting the uterine cavity.

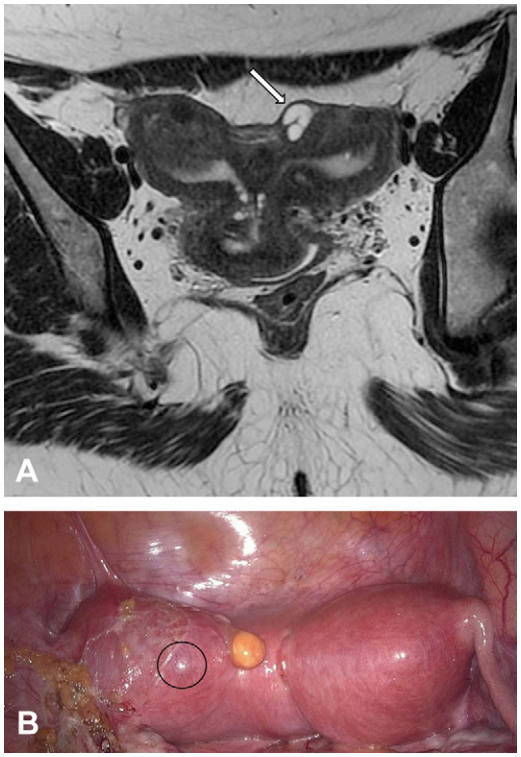

Figure 7. Cystic adenomyoma in a 42-year-old woman with Herlyn-Werner-Wunderlich syndrome. **(A)** Coronal T2-weighted MR image of the uterus shows a subserosal cystic lesion in the left hemiuterus (arrow). **(B)** Laparoscopic view shows the lesion (circle). (Courtesy of Ricardo M. A. Pereira, MD.)

leiomyomas include less-defined margins and minimal mass effect in adenomyomas. The presence of intralesional hemorrhagic foci can further support the likelihood of an adenomyoma because hemorrhagic degeneration in leiomyomas is rare and occurs more frequently in pregnant women (Fig S3).

Accurate differentiation between these entities is crucial in clinical practice to guide further management strategies (29). The differential diagnosis becomes more challenging with leiomyomas that exhibit hemorrhagic or cystic degeneration, which may contain central hyperintense areas at T1- or T2-weighted MRI, respectively. Another less common but important variant is the cellular leiomyoma, which typically shows low signal intensity at T1-weighted MRI, intermediate to high signal intensity at T2-weighted MRI, and restricted diffusion at diffusion-weighted MRI, usually with apparent diffusion coefficient (ADC) values higher than 0.9. Their pronounced contrast-enhanced patterns contribute to distinguishing them from adenomyosis (Fig S4) (33). Changes in the myometrium after myomectomy can also present diagnostic challenges (Fig S5).

Accessory Cavitated Uterine Mass.—ACUM, previously referred to as *juvenile cystic adenomyoma* or a *uterine-like mass*, is now considered a müllerian anomaly primarily linked to aberrant gubernaculum development (34,35). Acién et al (35) defined ACUM on the basis of three key features: *(a)* a noncommunicating accessory cavity lined with endometrium and surrounded by uterine smooth muscle; *(b)* a typical location in the anterolateral uterine wall near the round ligament insertion, exhibiting a uterus-like structure with dominant intramural and subserosal components; and *(c)* a normal appearance of the endometrial cavity, uterine fundus contour, fallopian tubes, and ovaries.

Patients with ACUM are usually nulliparous and younger than 30 years old, although cases of later onset have been documented (36). Clinically, it manifests with severe dysmenorrhea and chronic pelvic pain associated with endometrial function and intralesional bleeding during menstruation, typically starting a few years after menarche.

At imaging, ACUM typically appears as an intramural and subserosal nodular lesion with a central cavity filled with thick fluid showing ground-glass echogenicity on US images or signal hyperintensity on T1-weighted MR images. Doppler US may reveal peripheral blood flow, without any intralesional vascularity (37). It is frequently misdiagnosed as a degenerating intramural fibroid or a pseudo–broad ligament fibroid.

The ACUM wall consists of a well-organized smooth uterine myometrium that appears hypoechoic on US images and hypointense on T2-weighted MR images. The cavity is lined with a thin endometrial layer exhibiting mildly high signal intensity on T2-weighted MR images, resembling normal endometrial tissue. However, this endometrial lining may or may not be clearly visible on MR and US images (Fig 9).

Intramural Pregnancy.—Intramural pregnancy is an uncommon type of ectopic pregnancy situated in the uterine wall, enveloped by myometrium and separate from the uterine cavity, fallopian tubes, and round ligaments (38). It is marked by the gestational sac being eccentrically displaced toward the interstitial portion of the fallopian tube in the uterus. This condition should be suspected when an intramural cyst (with or without a fetal pole) accompanies elevated β-human chorionic gonadotropin levels and other sites for ectopic pregnancy have been ruled out. Early diagnosis is vital for initiating timely and appropriate management (Fig S6).

During pregnancy, cystic adenomyosis encircled by actively decidualized endometrial tissue exhibits thickened and

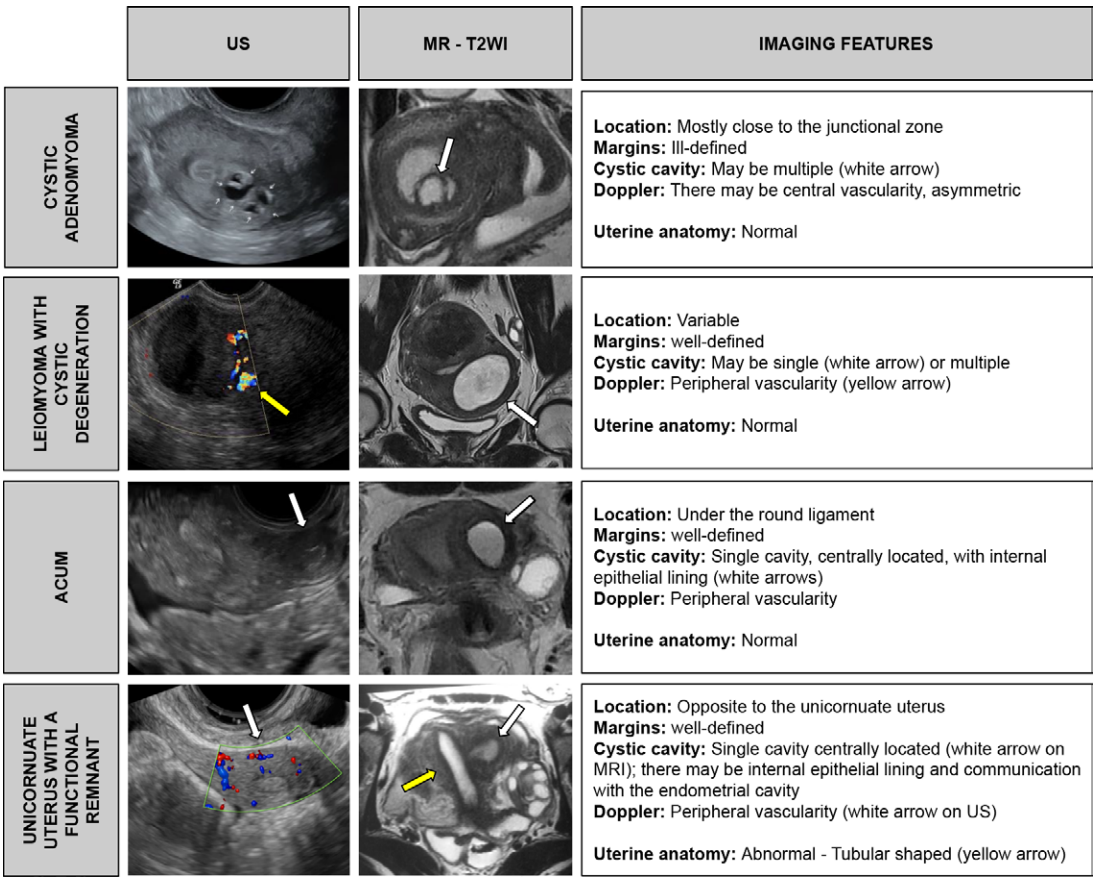

Figure 8. Tips for the differential diagnosis of cystic adenomyoma, leiomyoma with cystic degeneration, ACUM, and unicornuate uterus with a functional uterine remnant. *T2WI* = T2-weighted MRI.

echogenic cyst walls that mimic the trophoblastic echogenicity seen in early gestational sacs. This manifestation in early pregnancy may be mistaken for intramural gestational sac implantation (39). Examining pelvic imaging studies conducted before pregnancy can assist in delineating the previous distribution of adenomyosis, thereby aiding in the differentiation of these conditions. US is the primary diagnostic modality for intramural pregnancy, while MRI may be indicated for confirmation in equivocal cases and to assist in surgical planning (38).

Adenomatoid Tumors.—Adenomatoid tumors are rare benign mesenchymal tumors that presumably originated in mesothelial cells of the uterine serosa (40). They are usually found incidentally in surgical specimens from hysterectomy. There are four described histologic types that affect imaging findings: adenoid, angiomatoid, solid, and cystic types (41). Combinations of two or more patterns can occur (41).

Most cases manifest as nodular lesions measuring 0.5–1.0 cm on the periphery of the uterus, potentially with firm adherence to local structures (40). The primary conditions to consider in the differential diagnosis include fibroids and their malignant forms. Rarely, adenomatoid tumors manifest as multiloculated cysts (41), posing a challenge in distinguishing them from cystic adenomyomas. Microscopically, adenomatoid tumors are characterized by networks of tubules covered by mesothelial cells, with interposed muscle fibers and a concentric or disorganized appearance.

Radiologic features that support the diagnosis of adenomatoid tumors include their location, typically in the outer myometrium or subserosa (often in the fundus); ill-defined borders; heterogeneous hypoenhancement compared with the myometrium; and the absence of necrosis and hemorrhage.

Extrauterine Adenomyomas

Extrauterine adenomyoma is a controversial entity, and few cases have been reported in the literature to date and to our knowledge (42). As depicted in Figure 10, there are rare and challenging manifestations of pelvic masses containing heterotopic endometrial tissue outside the uterus that cannot be classified as endometriosis or other conditions considered as part of its common differential diagnosis.

Batt et al (43) proposed the terminology *müllerian choristomas*, which are defined as organoid proliferations of normal tissue or soft nodules of embryonic origin found in aberrant anatomic locations. Müllerian choristomas have been reported in both pelvic and extrapelvic sites and may contain one, two, or all three müllerian components: endocervix, endometrium, and endosalpinx (43).

Müllerian choristomas can be definitively diagnosed under three conditions: *(a)* the absence of pelvic endometriosis; *(b)* the lack of direct connections with the endocervix, endometrium, or endosalpinx; and *(c)* the lack of a history of reproductive organ surgery that could have caused inadvertent displacement of these tissue cells to heterotopic sites (43). Radiologically, they may appear as lobulated heterogeneous pelvic masses with intervening cystic components, some of which may contain hemorrhagic content. Once they are

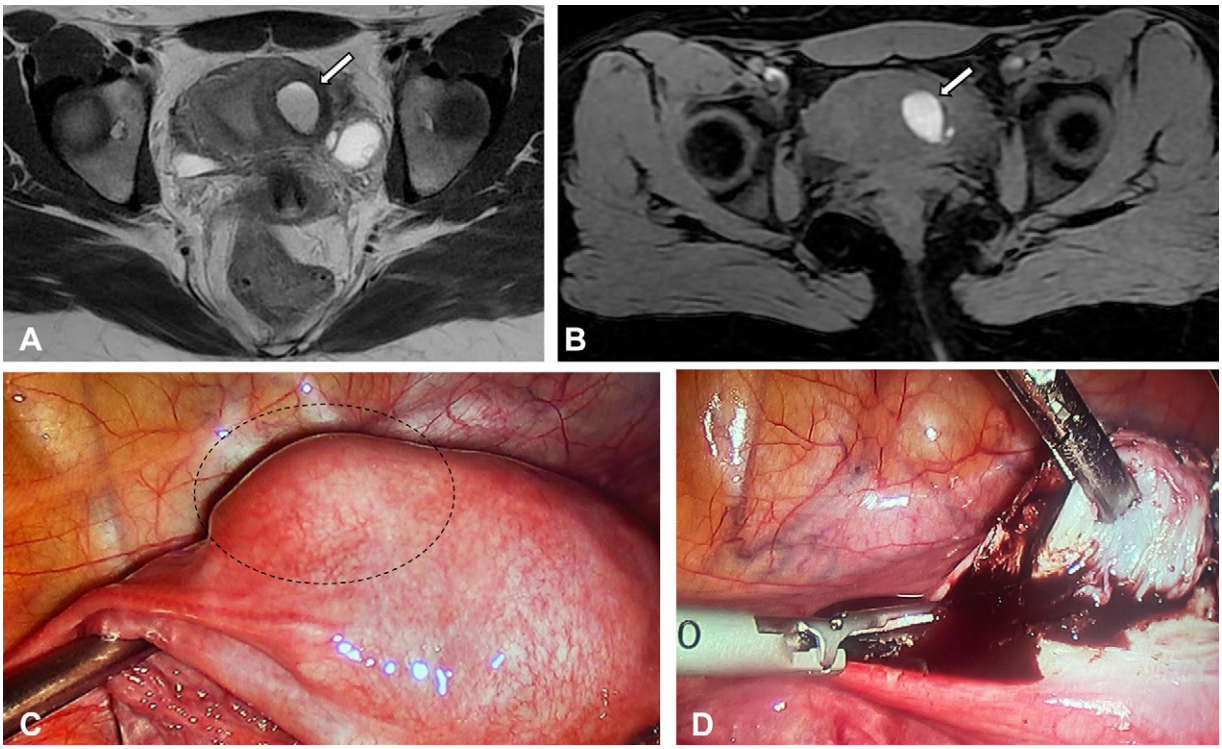

Figure 9. ACUM in a 14-year-old nulliparous adolescent girl with intense dysmenorrhea since menarche. **(A)** Axial T2-weighted MR image shows a cystic cavity lined with endometrium and surrounded by a hypointense halo in the left uterine body (arrow). **(B)** Axial T1-weighted MR image with fat saturation shows prominent high signal intensity in the central cavity, corresponding to hemorrhagic content (arrow). **(C)** Laparoscopic surgical view shows the mass on the left side of the uterus, bulging the organ (dashed circle). **(D)** Laparoscopic surgical view shows a section of the mass with chocolate-colored fluid spilling out. (Courtesy of Homero Leal Meirelles, Jr., MD.)

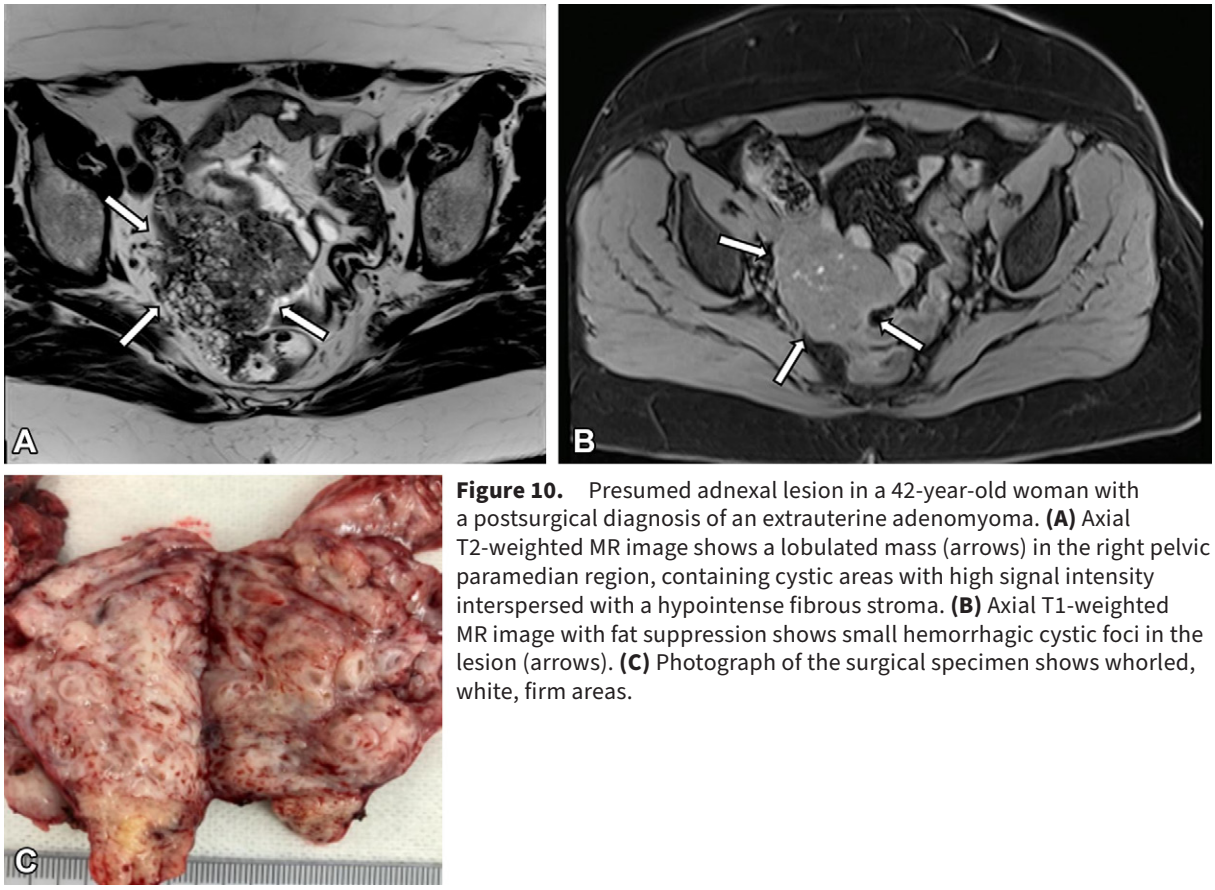

Figure 10. Presumed adnexal lesion in a 42-year-old woman with a postsurgical diagnosis of an extrauterine adenomyoma. **(A)** Axial T2-weighted MR image shows a lobulated mass (arrows) in the right pelvic paramedian region, containing cystic areas with high signal intensity interspersed with a hypointense fibrous stroma. **(B)** Axial T1-weighted MR image with fat suppression shows small hemorrhagic cystic foci in the lesion (arrows). **(C)** Photograph of the surgical specimen shows whorled, white, firm areas.

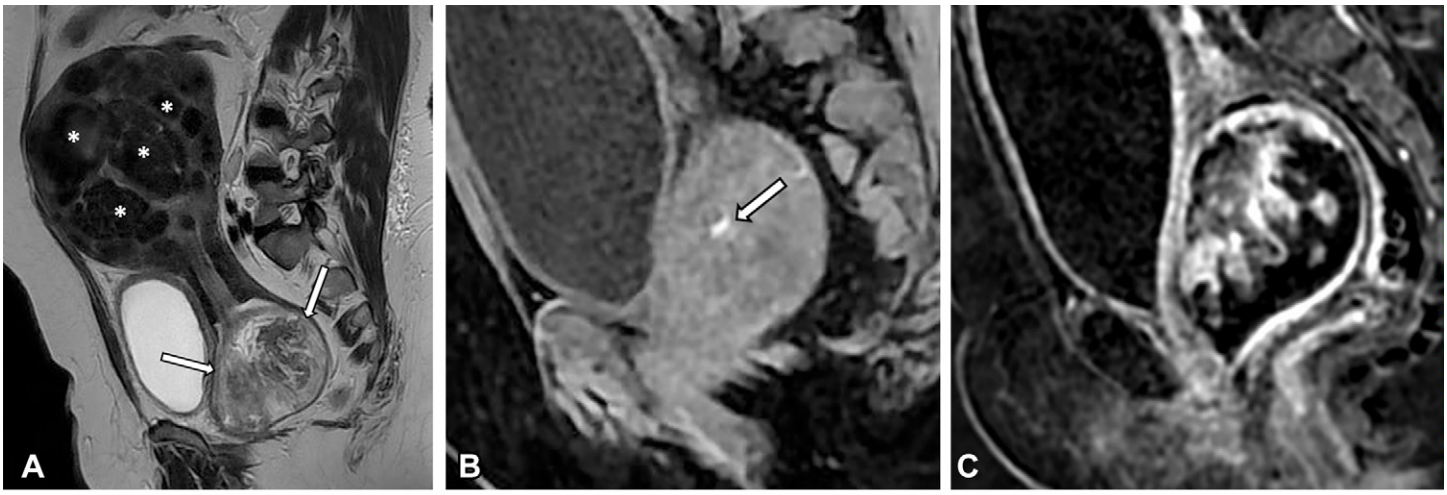

Figure 11. Atypical polypoid adenoma in a 50-year-old woman. **(A)** Sagittal T2-weighted MR image shows an enlarged uterus with multiple hypointense masses representing leiomyomas (∗) and a polypoid lesion anchored in the lower uterine segment, protruding into the vagina (arrows). **(B)** Sagittal T1-weighted MR image with fat suppression shows a small hemorrhagic focus in the lesion (arrow). **(C)** Sagittal postcontrast MR image shows irregular areas of enhancement. **(D)** Diffusion-weighted MR image shows peripheral restriction (arrows).

diagnosed, müllerian choristomas can be surgically excised, providing definitive treatment of a nonrecurrent condition (44).

Polypoid Adenomyoma

An adenomyoma that protrudes into the endometrial cavity is known as a polypoid adenomyoma. Its stromal component consists of smooth muscle. Typically, a polypoid adenomyoma occurs in infertile patients (median age, 35–40 years) with polypoid lesions arising on the inferior uterine segment (22–24). These tumors are rare and can be classified into typical and atypical types on the basis of their histopathologic features. Atypical polypoid adenomyomas are distinguished by the presence of endometrial glands showing varying degrees of atypia within a myofibromatous stroma (Fig 11) (45).

On hysteroscopic images, polypoid adenomyomas closely resemble conventional endometrial polyps and submucosal intracavitary fibroids, but they may exhibit distinguishing imaging features (Table 4) (Fig S7). According to US findings (45), patterns of polypoid adenomyoma can be classified as follows, in order of frequency of occurrence: *(a)* a solid polypoid mass containing multiple small (<0.3 cm) or large cysts, some of which may show echogenic fluid (indicating hemorrhagic content); *(b)* a completely solid mass consisting of smooth muscle stroma, with low homogeneous echogenicity (in comparison to that of endometrial polyps, which are typically hyperechoic); and *(c)* a well-defined cystic mass containing anechoic or echogenic fluid (Fig 12).

At MRI, polypoid adenomyomas appear as well-defined intracavitary uterine masses that can involve the lower uterine segment, the endocervix, or the uterine corpus. The "broccoli sign" refers to a stalk connecting a cervical mass to the endometrial cavity, indicating a prolapsed uterine tumor. Signal intensity on T2-weighted MR images may vary depending on the amount of hemorrhage in cystic spaces, which appear as hyperintense foci on T1-weighted MR images. Polypoid adenomyomas generally do not exhibit diffusion restriction and enhance heterogeneously, typically less than the myometrium does (Figs 13, 14) (45).

Conservative management through operative hysteroscopy is recommended, with close follow-up considered for patients aiming to preserve fertility, reduce recurrence rates, and enhance the accuracy of diagnosing concurrent endometrial cancer. Hysterectomy is indicated for perimenopausal or postmenopausal patients (46).

Adenomyosis during Pregnancy

During pregnancy, adenomyosis often undergoes hormonal changes, primarily influenced by progesterone and other complex molecular pathways that induce decidualization of the endometrium. Differentiating adenomyosis from normal and abnormal decidualization can be challenging, particularly when adenomyosis is located beneath the placenta, due to the blurred boundary between them, as well as their overlapping imaging features (Figs 15, 16) (16).

During the first trimester of pregnancy, decidualization may lead to wall thickening and an increase in the number and size of myometrial cysts associated with adenomyosis. This imaging appearance may mimic gestational trophoblastic disease, including a complete or partial hydatidiform mole (15).

Furthermore, failure to distinguish between adenomyosis and the placenta as distinct entities can lead to misdiagnosis of conditions such as mesenchymal dysplasia, which is characterized by heterogeneous cystic enlargement of the

Table 4: Clinical and Imaging Features of Polypoid Adenomyomas, Submucosal Intracavitary Fibroids, and Endometrial Polyps

Characteristic	Polypoid Adenomyoma	Submucosal Intracavitary Fibroids	Endometrial Polyps
Epidemiology	Rare, often in women of reproductive age	Common in women of reproductive age	Frequently occur in postmenopausal women
US	Isoechoic to myometrium, heterogeneous	Hypoechoic	Hyperechoic
T1-weighted MRI	Isointense to myometrium	Isointense to myometrium	Isointense or slightly hypointense
T2-weighted MRI	Hyperintense to myometrium, heterogeneous	Hypointense	Hyperintense (central) and hypointense (peripheral)
Calcification	Rare	Common in women with older fibroids	Rare
Necrosis and cysts	Cysts with hemorrhagic content are common	Rare, usually associated with degeneration	Rare cysts, with simple fluid

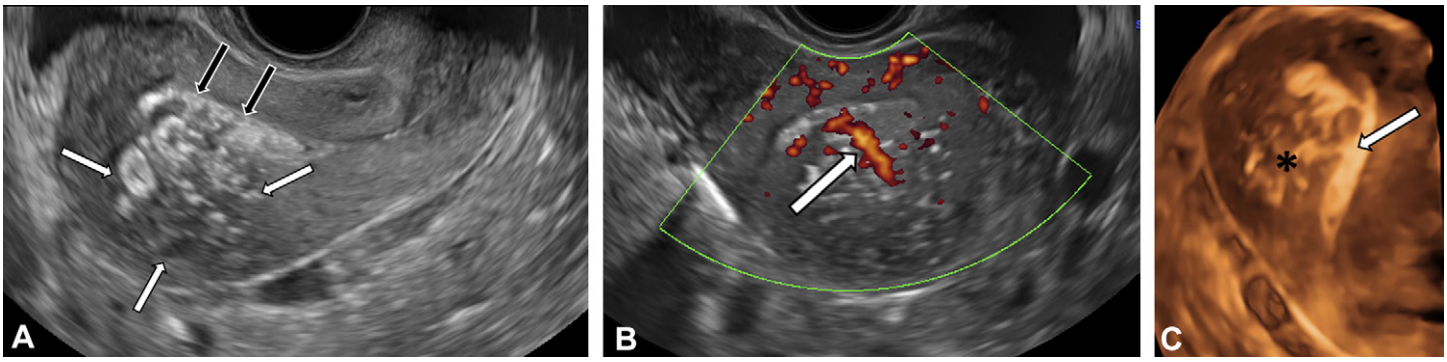

Figure 12. Polypoid adenomyoma in an asymptomatic 40-year-old woman who was taking hormone therapy. **(A)** Longitudinal endovaginal US image shows diffuse adenomyosis in the posterior uterine wall (white arrows) continuous with a hyperechoic polypoid lesion (black arrows). **(B)** Doppler endovaginal US image shows the vascular pedicle (arrow), which originates from the area of adenomyosis. **(C)** Sagittal three-dimensional surface-rendered US image shows the hyperechoic lesion (arrow) attached to the site of adenomyosis (*).

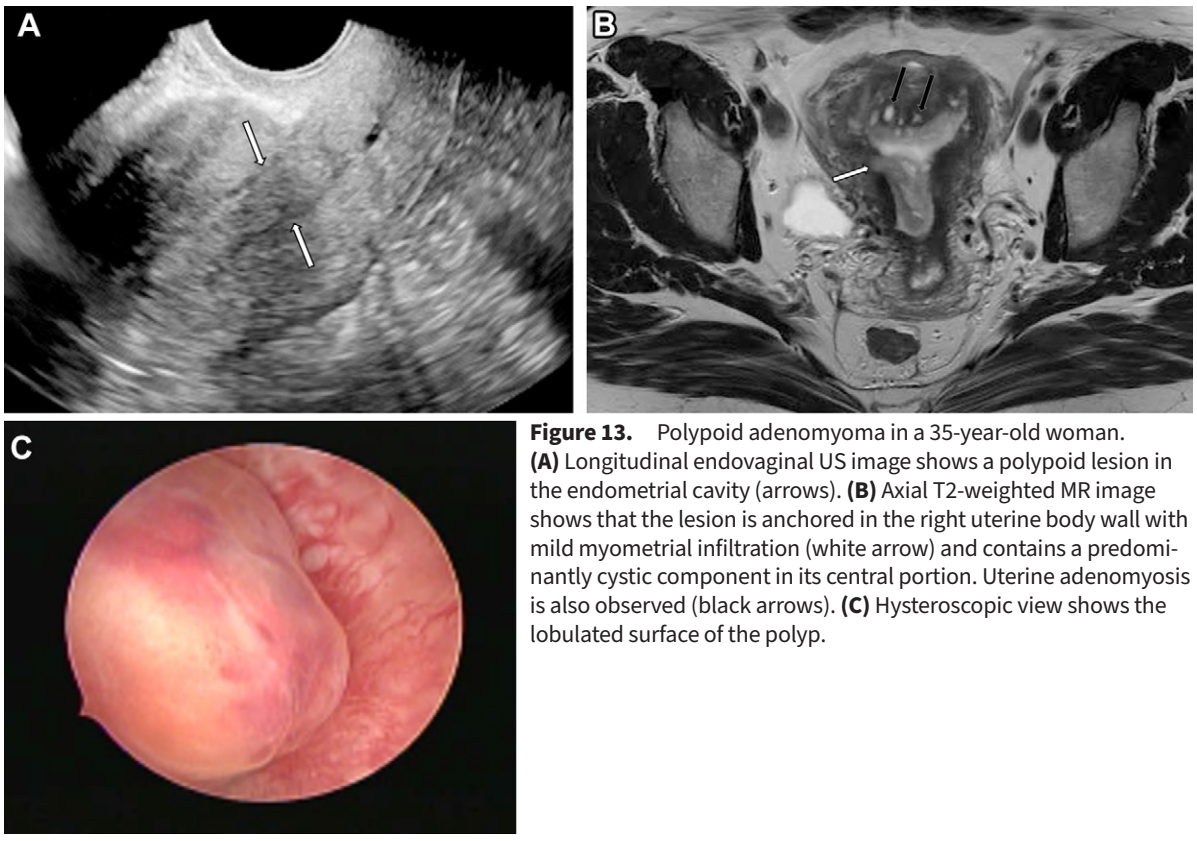

Figure 13. Polypoid adenomyoma in a 35-year-old woman. **(A)** Longitudinal endovaginal US image shows a polypoid lesion in the endometrial cavity (arrows). **(B)** Axial T2-weighted MR image shows that the lesion is anchored in the right uterine body wall with mild myometrial infiltration (white arrow) and contains a predominantly cystic component in its central portion. Uterine adenomyosis is also observed (black arrows). **(C)** Hysteroscopic view shows the lobulated surface of the polyp.

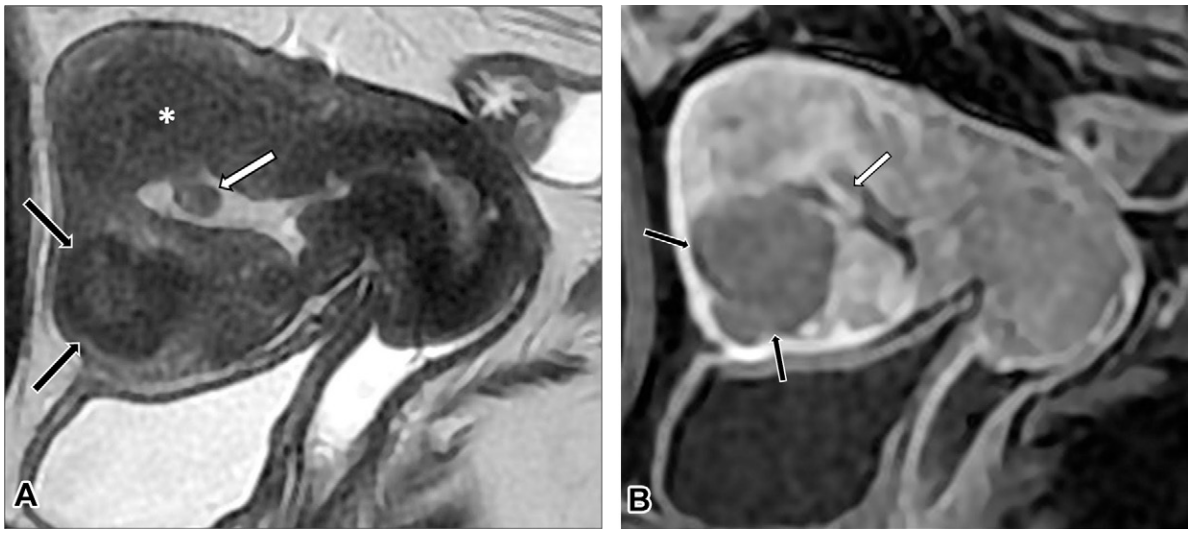

Figure 14. Polypoid adenomyoma in a 45-year-old woman. **(A)** Sagittal T2-weighted MR image shows a polypoid lesion (white arrow) in the uterine cavity, with small internal cystic areas, accompanied by diffuse adenomyosis of the posterior uterine wall (∗) and an intramural leiomyoma in the anterior wall (black arrows). **(B)** Sagittal T1-weighted contrast-enhanced MR image with fat saturation shows the highly enhancing polypoid lesion (white arrow) and the low enhancement of the hyalinized leiomyoma (black arrows).

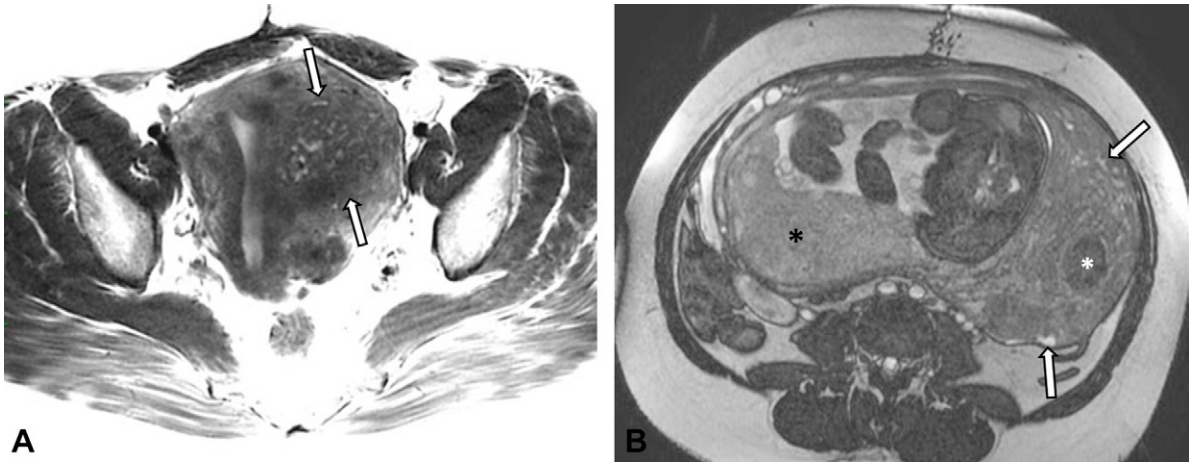

Figure 15. Adenomyosis before and during pregnancy in the same patient. **(A)** Pregravid axial T2-weighted MR image in a 33-year-old woman shows a hypointense intramyometrial mass in the left uterine wall with partially defined margins, minimal mass effect, and small internal hyperintense foci, which are findings characteristic of an adenomyoma (arrows). **(B)** Axial T2-weighted MR image during the third trimester of pregnancy when the patient was 36 years old shows a heterogeneously thickened left myometrium with scattered cystic areas (arrows). A normal placenta (black ∗) and an additional finding of a leiomyoma (white ∗) are also visible. (Case courtesy of Patrícia Prando, MD, PhD.)

placenta, a rare but serious condition associated with prenatal complications and linked with Beckwith-Wiedemann syndrome in 20% of cases (16). In addition, adenomyosis without cystic components can also mimic disorders on the placenta accreta spectrum, in which the placenta abnormally attaches to or invades into the myometrium, carrying substantial morbidity and mortality rates and often requiring complex resource-intensive multidisciplinary treatment (Fig S8) (16).

In some cases, using a lower-frequency US probe may help to distinguish between placental and myometrial echogenicity, particularly when the placenta is located posteriorly, owing to its superior penetration ability (16). Moreover, on color Doppler US images, adenomyosis typically shows increased and diffuse blood flow in the affected region, with normal subplacental vessels that run parallel to the placental attachment (16).

Comparing gestational pelvic US images with previous imaging studies can aid in correlating the distribution of adenomyosis. If abnormalities remain ambiguous, nonenhanced MRI can provide improved tissue contrast to differentiate the placenta-myometrial interface (16).

Adenomyosis has been associated with adverse obstetric outcomes such as increased risks of spontaneous abortion, premature birth, restricted intrauterine growth, hypertension, and placental abruption. Therefore, its management should be conducted in a high-risk obstetric unit (40). Accurately diagnosing decidualized adenomyosis helps prevent unnecessary investigations and reduces patient anxiety (16).

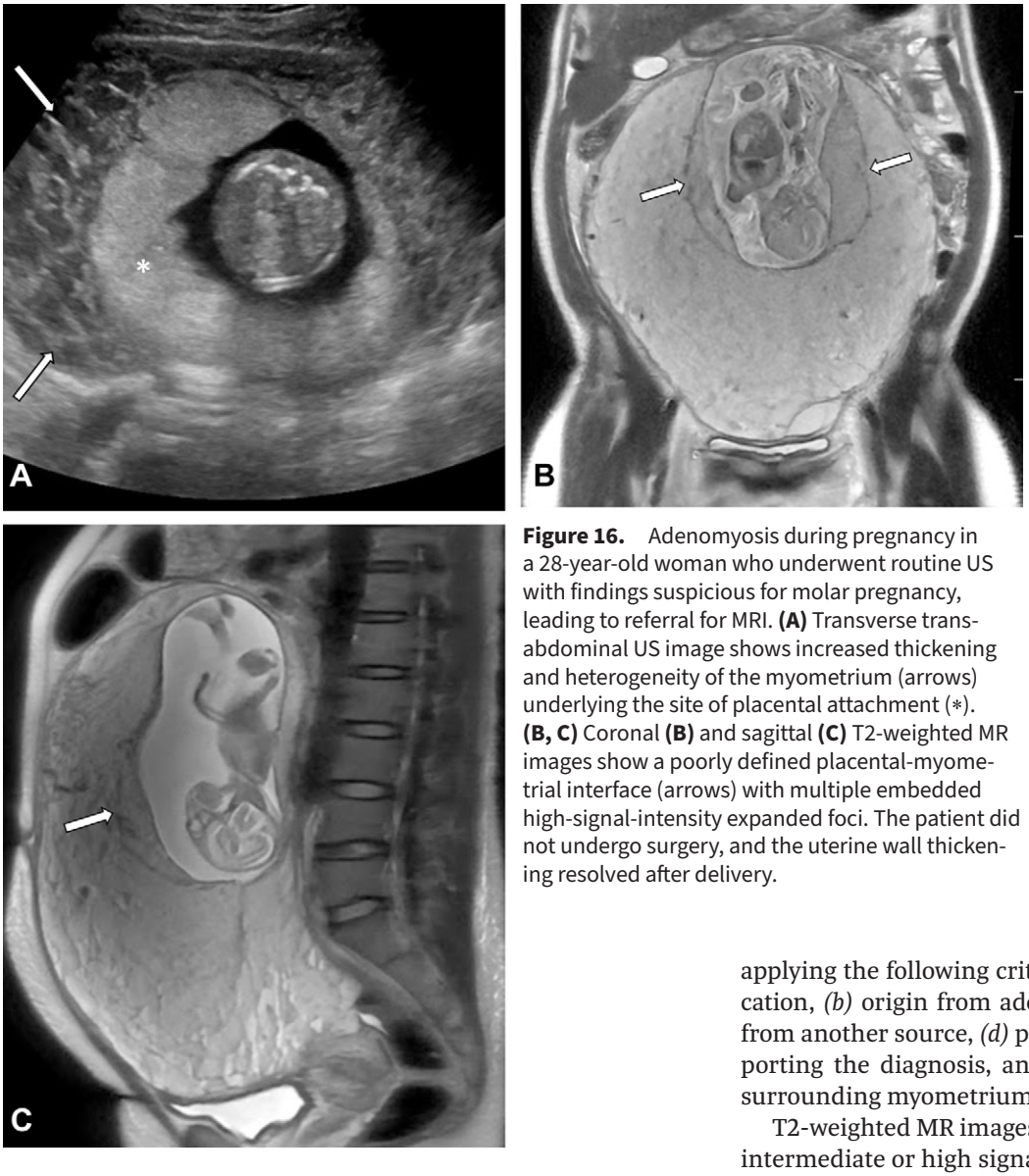

Figure 16. Adenomyosis during pregnancy in a 28-year-old woman who underwent routine US with findings suspicious for molar pregnancy, leading to referral for MRI. **(A)** Transverse transabdominal US image shows increased thickening and heterogeneity of the myometrium (arrows) underlying the site of placental attachment (*). **(B, C)** Coronal **(B)** and sagittal **(C)** T2-weighted MR images show a poorly defined placental-myometrial interface (arrows) with multiple embedded high-signal-intensity expanded foci. The patient did not undergo surgery, and the uterine wall thickening resolved after delivery.

Malignant Transformation of Adenomyosis

Malignant transformation of adenomyosis is rare, occurring in only 1% of cases. The exact pathogenic mechanism remains unclear, but it may involve prolonged exposure to elevated estrogen levels, immune system activation and dysregulation, inflammation, molecular changes, and treatment with tamoxifen and radiation therapy (47,48). The most commonly associated cancers are endometrioid carcinoma, clear cell carcinoma, adenosarcoma, carcinosarcoma, and müllerian mucinous borderline tumor (49).

Most cases occur in postmenopausal patients, and symptoms often overlap with those of adenomyosis, including abnormal vaginal bleeding, menorrhagia, anemia, and weight loss (50). The expression of the tumor markers CA 125 and CA 19–9 may be increased. Malignant transformation may coexist with polypoid lesions that protrude in the cavity and endometrial cancer.

No definitive endovaginal US or MRI findings indicate malignant transformation. Diagnosis often relies on comparing current imaging studies with previous examinations and applying the following criteria: *(a)* suspicious myometrial location, *(b)* origin from adenomyosis, *(c)* absence of invasion from another source, *(d)* presence of adenomyotic tissue supporting the diagnosis, and *(e)* adenomyotic changes in the surrounding myometrium (49).

T2-weighted MR images may show a myometrial area with intermediate or high signal intensity inside the adenomyotic lesion or a solid papillary projection in a cystic subserosal adenomyoma (51). Malignant lesions are usually isointense on T1-weighted MR images and enhance after gadolinium-based contrast material is injected (Fig 17). Restricted diffusion manifesting as hyperintensity on diffusion-weighted MR images and hypointensity on apparent diffusion coefficient maps suggests malignant transformation but does not occur in all cases (51). In patients in whom malignancy is suspected on the basis of imaging findings, hysterectomy is recommended for histologic confirmation.

Endometrial Adenocarcinoma

Endometrial cancer arising from adenomyosis is rare, but the coexistence of endometrial adenocarcinoma and adenomyosis in the same uterus is common (26,52,53). Endometrial carcinoma usually manifests with homogeneous signal isointensity to the endometrium on T2-weighted MR images and signal hyperintensity on diffusion-weighted MR images, in contrast to adenomyosis, and is rarely associated with cysts and bleeding.

Adenomyosis can make the endometrial–myometrial border indistinct, reducing the precision of MRI-based

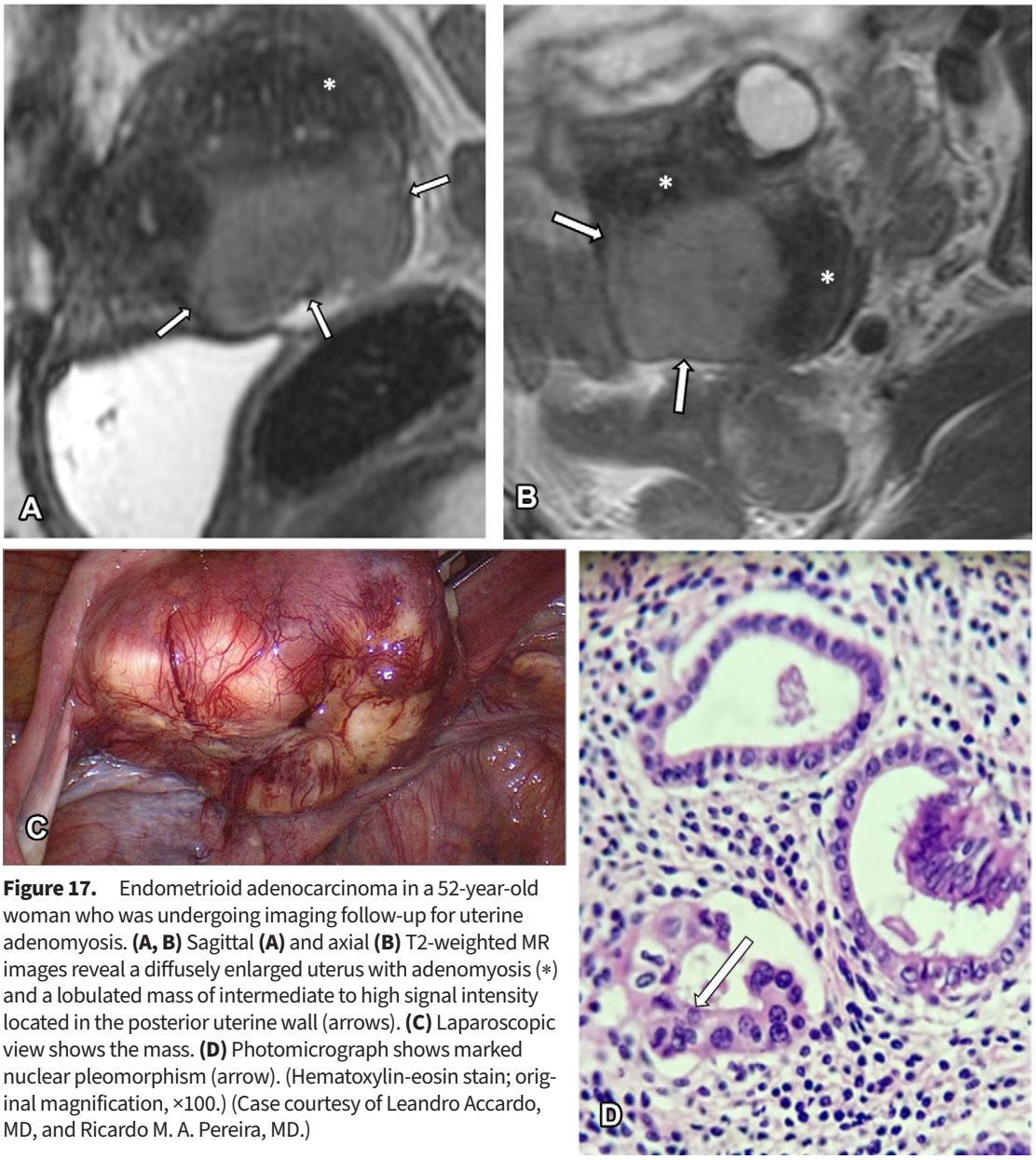

Figure 17. Endometrioid adenocarcinoma in a 52-year-old woman who was undergoing imaging follow-up for uterine adenomyosis. **(A, B)** Sagittal **(A)** and axial **(B)** T2-weighted MR images reveal a diffusely enlarged uterus with adenomyosis (*) and a lobulated mass of intermediate to high signal intensity located in the posterior uterine wall (arrows). **(C)** Laparoscopic view shows the mass. **(D)** Photomicrograph shows marked nuclear pleomorphism (arrow). (Hematoxylin-eosin stain; original magnification, ×100.) (Case courtesy of Leandro Accardo, MD, and Ricardo M. A. Pereira, MD.)

evaluation of the depth of the endometrial adenocarcinoma invasion (51). It can also mimic invasion of endometrial carcinoma because it causes "pseudowidening" of the endometrium related to the invasion of the myometrium by the basal endometrium. In a patient with endometrial adenocarcinoma, these findings can be mistaken as myometrial invasion.

Low-grade Endometrial Stromal Sarcoma

Low-grade endometrial stromal sarcoma is a lesion arising from the cells of the endometrial stroma. It can originate in the endometrium, in adenomyosis, and occasionally in endometriosis (54). Compared with other uterine malignancies, low-grade endometrial stromal sarcoma tends to manifest before menopause (mean age, 39 years) and grows slowly (54). Low-grade endometrial stromal sarcoma most commonly grows from the uterine endometrium into the endometrial cavity and rarely is located in the myometrium, where it may resemble cystic adenomyosis or a degenerated leiomyoma.

The US and MRI features are nonspecific for the diagnosis of endometrial stromal sarcoma because similar changes may be seen in endometrial carcinoma, undifferentiated carcinoma, and adenosarcoma. Nevertheless, certain MRI characteristics, such as smooth and well-defined margins at baseline MRI, the presence of cystic and solid components with high signal intensity at T2-weighted MRI, substantial contrast enhancement, and a thin low-intensity rim, may suggest low-grade endometrial stromal sarcoma (54) (Fig 18).

Conclusion

Adenomyosis manifests with typical and several atypical imaging features, which can be challenging for radiologists and clinicians. Although various classification systems for adenomyosis exist, none have achieved widespread clinical acceptance. It is crucial to comprehend these common and uncommon manifestations and the conditions to consider in

Figure 18. Adenomyosis in a 46-year-old woman with confirmed low-grade endometrial stromal sarcoma. **(A, B)** Axial **(A)** and sagittal **(B)** T2-weighted MR images show a large myometrial cystic mass abutting the uterine cavity (arrows). **(C, D)** Axial **(C)** and sagittal **(D)** T2-weighted MR images acquired 3 years later show substantial growth of the lesion (arrows), which exhibits prominent high signal intensity and a peripheral hypointense component (∗) corresponding to solid areas or clots . The patient did not receive intravenous contrast material due to a history of allergy. **(E)** Photograph of the surgical specimen shows the mass (∗). (Case courtesy of Renata Laranjeira, MD, and Marco Aurélio Lameirão, MD.)

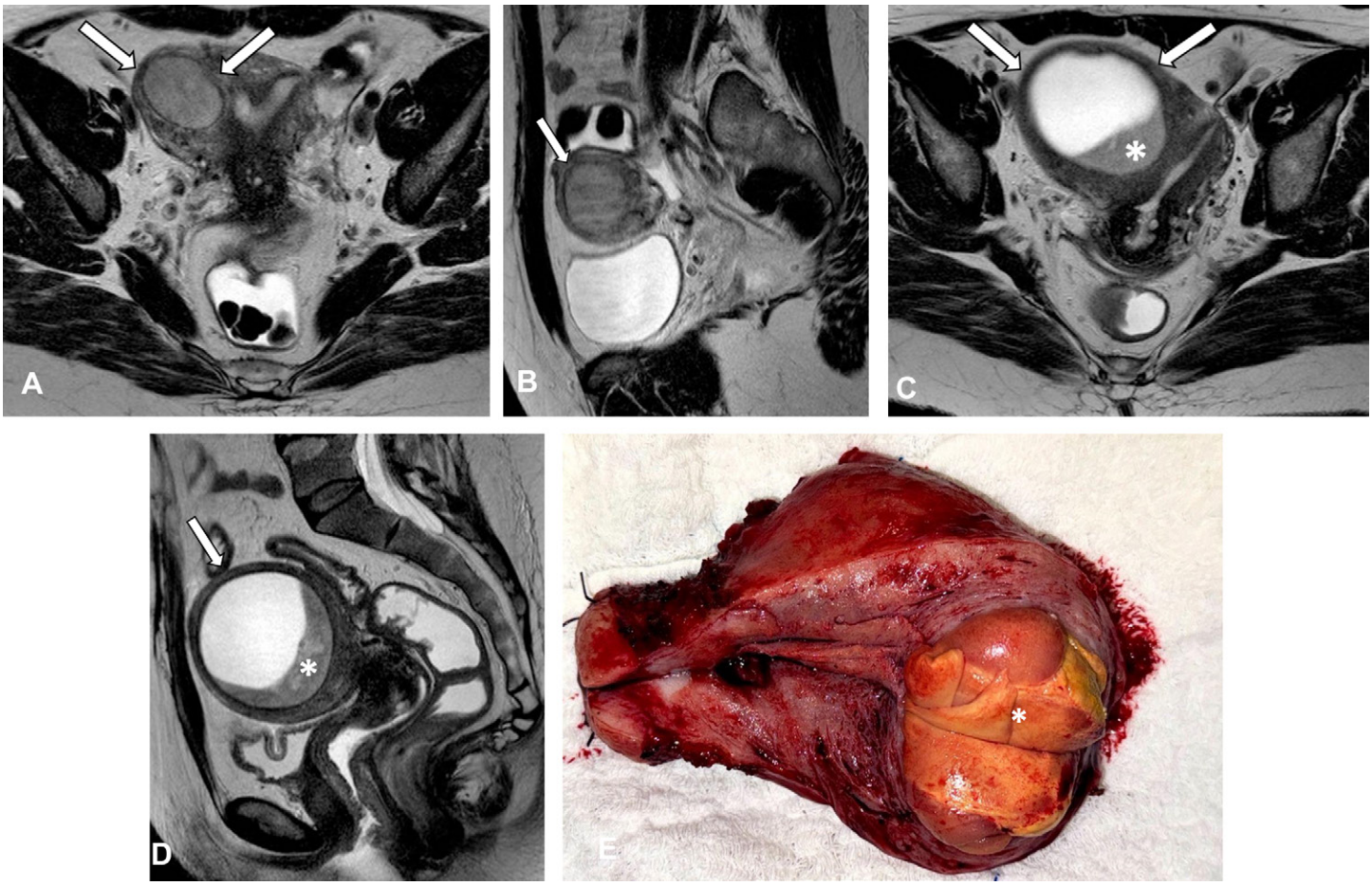

the differential diagnosis to enhance clinical treatment and reproductive outcomes in affected patients.

Author affiliations.—From the Fonte Imagem Medicina Diagnóstica, Rua Fonte da Saudade, 277, Rio de Janeiro, RJ 22471-211, Brazil (A.B., I.A.G.F., L.B.); Chamié Imagem da Mulher, São Paulo, Brazil (B.C.O., L.P.C.); Clínica Matteoni de Athayde, Salvador, Brazil (L.G.M.A.); Fleury Medicina e Saúde, São Paulo, Brazil (L.R.T.); Instituto Nacional de Câncer, Rio de Janeiro, Brazil (L.B.); Clínica Izabela Pires Franco, Belém, Brazil (I.P.F.); and Department of Radiology and Imaging Sciences, University of Utah, Salt Lake City, Utah (A.M.S., D.R.). Presented as an education exhibit at the 2023 RSNA Annual Meeting. Received May 2, 2024; revision requested May 28 and received July 9; accepted July 16. **Address correspondence to** A.B. (email: *brandaosalomao@gmail.com*).

Disclosures of conflicts of interest.—All authors, the editor, and the reviewers have disclosed no relevant relationships.

References

1. Shruthi A, Sreelatha S, Kumar S, Kavita BL. Adenomyosis in patients undergoing hysterectomy for leiomyomas: A retrospective study. International Journal of Clinical Obstetrics and Gynaecology. https://www.gynaecologyjournal.com/articles/74/2-2-14-642.pdf. Published 2018. Accessed December 5, 2024.
2. Mishra I, Melo P, Easter C, Sephton V, Dhillon-Smith R, Coomarasamy A. Prevalence of adenomyosis in women with subfertility: systematic review and meta-analysis. Ultrasound Obstet Gynecol 2023;62(1):23–41.
3. Bergeron C. Histologie et physiologie de l'endomètre normal. EMC - Gynécologie 2006;1(3):1–8.
4. Chapron C, Tosti C, Marcellin L, et al. Relationship between the magnetic resonance imaging appearance of adenomyosis and endometriosis phenotypes. Hum Reprod 2017;32(7):1393–1401.
5. Chapron C, Vannuccini S, Santulli P, et al. Diagnosing adenomyosis: an integrated clinical and imaging approach. Hum Reprod Update 2020;26(3):392–411.
6. Leyendecker G, Bilgicyildirim A, Inacker M, et al. Adenomyosis and endometriosis. Re-visiting their association and further insights into the mechanisms of auto-traumatisation. An MRI study. Arch Gynecol Obstet 2015;291(4):917–932.
7. Levgur M, Abadi MA, Tucker A. Adenomyosis: symptoms, histology, and pregnancy terminations. Obstet Gynecol 2000;95(5):688–691.
8. Panganamamula UR, Harmanli OH, Isik-Akbay EF, Grotegut CA, Dandolu V, Gaughan JP. Is prior uterine surgery a risk factor for adenomyosis? Obstet Gynecol 2004;104(5 Pt 1):1034–1038.
9. Vavilis D, Agorastos T, Tzafetas J, et al. Adenomyosis at hysterectomy: prevalence and relationship to operative findings and reproductive and menstrual factors. Clin Exp Obstet Gynecol 1997;24(1):36–38.
10. Bergholt T, Eriksen L, Berendt N, Jacobsen M, Hertz JB. Prevalence and risk factors of adenomyosis at hysterectomy. Hum Reprod 2001;16(11):2418–2421.
11. Campo S, Campo V, Benagiano G. Infertility and adenomyosis. Obstet Gynecol Int 2012;2012:786132.
12. Younes G, Tulandi T. Effects of adenomyosis on in vitro fertilization treatment outcomes: a meta-analysis. Fertil Steril 2017;108(3):483–490.e3.
13. Park CW, Choi MH, Yang KM, Song IO. Pregnancy rate in women with adenomyosis undergoing fresh or frozen embryo transfer cycles following gonadotropin-releasing hormone agonist treatment. Clin Exp Reprod Med 2016;43(3):169–173.

14. Moawad G, Fruscalzo A, Youssef Y, et al. Adenomyosis: An Updated Review on Diagnosis and Classification. J Clin Med 2023;12(14):4828.
15. Takeuchi M, Matsuzaki K. Adenomyosis: usual and unusual imaging manifestations, pitfalls, and problem-solving MR imaging techniques. RadioGraphics 2011;31(1):99–115.
16. Jensen KK, Pyle C, Foster BR, Sohaey R, Oh KY. Adenomyosis in pregnancy: Diagnostic pearls and pitfalls. RadioGraphics 2021;41(3):929–944.
17. Gordts S, Grimbizis G, Campo R. Symptoms and classification of uterine adenomyosis, including the place of hysteroscopy in diagnosis. Fertil Steril 2018;109(3):380-388.e1.
18. Andres MP, Borrelli GM, Ribeiro J, Baracat EC, Abrão MS, Kho RM. Transvaginal Ultrasound for the Diagnosis of Adenomyosis: Systematic Review and Meta-Analysis. J Minim Invasive Gynecol 2018;25(2):257–264.
19. Van den Bosch T, de Bruijn AM, de Leeuw RA, et al. Sonographic classification and reporting system for diagnosing adenomyosis. Ultrasound Obstet Gynecol 2019;53(5):576–582.
20. Harmsen MJ, Van den Bosch T, de Leeuw RA, et al. Consensus on revised definitions of Morphological Uterus Sonographic Assessment (MUSA) features of adenomyosis: results of modified Delphi procedure. Ultrasound Obstet Gynecol 2022;60(1):118–131.
21. Bazot M, Daraï E. Role of transvaginal sonography and magnetic resonance imaging in the diagnosis of uterine adenomyosis. Fertil Steril 2018;109(3):389–397.
22. Tong A, VanBuren WM, Chamié L, et al. Recommendations for MRI technique in the evaluation of pelvic endometriosis: consensus statement from the Society of Abdominal Radiology endometriosis disease-focused panel. Abdom Radiol (NY) 2020;45(6):1569–1586.
23. Bazot M, Bharwani N, Huchon C, et al. European society of urogenital radiology (ESUR) guidelines: MR imaging of pelvic endometriosis. Eur Radiol 2017;27(7):2765–2775.
24. Celli V, Dolciami M, Ninkova R, et al. MRI and Adenomyosis: What Can Radiologists Evaluate? Int J Environ Res Public Health 2022;19(10):5840.
25. Li X, Liu X, Guo SW. Clinical profiles of 710 premenopausal women with adenomyosis who underwent hysterectomy. J Obstet Gynaecol Res 2014;40(2):485–494.
26. Agostinho L, Cruz R, Osório F, Alves J, Setúbal A, Guerra A. MRI for adenomyosis: a pictorial review. Insights Imaging 2017;8(6):549–556..
27. Kobayashi H, Matsubara S. A Classification Proposal for Adenomyosis Based on Magnetic Resonance Imaging. Gynecol Obstet Invest 2020;85(2):118–126.
28. Tellum T, Matic GV, Dormagen JB, et al. Diagnosing adenomyosis with MRI: a prospective study revisiting the junctional zone thickness cutoff of 12 mm as a diagnostic marker. Eur Radiol 2019;29(12):6971–6981.
29. Baba A, Yamazoe S, Dogru M, Ogawa M, Takamatsu K, Miyauchi J. Clear cell adenocarcinoma arising from adenomyotic cyst: A case report and literature review. J Obstet Gynaecol Res 2016;42(2):217–223.
30. Tamai K, Togashi K, Ito T, Morisawa N, Fujiwara T, Koyama T. MR imaging findings of adenomyosis: Correlation with histopathologic features and diagnostic pitfalls. RadioGraphics 2005;25(1):21–40.
31. Zhang M, Bazot M, Tsatoumas M, Munro MG, Reinhold C. MRI of Adenomyosis: Where Are We Today? Can Assoc Radiol J 2023;74(1):58–68.
32. Marcellin L, Santulli P, Bourdon M, et al. Focal adenomyosis of the outer myometrium and deep infiltrating endometriosis severity. Fertil Steril 2020;114(4):818–827.
33. Nakai G, Matsutani H, Yamada T, Ohmichi M, Yamamoto K, Osuga K. Imaging findings of uterine adenosarcoma with sarcomatous overgrowth: two case reports, emphasizing restricted diffusion on diffusion weighted imaging. BMC Womens Health 2021;21(1):416.
34. Acién P, Sánchez del Campo F, Mayol MJ, Acién M. The female gubernaculum: role in the embryology and development of the genital tract and in the possible genesis of malformations. Eur J Obstet Gynecol Reprod Biol 2011;159(2):426–432.
35. Acién P, Acién M, Fernández F, José Mayol M, Aranda I. The cavitated accessory uterine mass: a Müllerian anomaly in women with an otherwise normal uterus. Obstet Gynecol 2010;116(5):1101–1109.
36. Brosens I, Gordts S, Habiba M, Benagiano G. Uterine Cystic Adenomyosis: A Disease of Younger Women. J Pediatr Adolesc Gynecol 2015;28(6):420–426.
37. Shah MV, Pisat S, Jain M, Chatterjee M, Nadkarni S, Bijlani S. Role of 3D Coronal Ultrasound in Diagnosis of Accessory and Cavitated Uterine Mass: A rare Müllerian Anomaly. J Obstet Gynaecol India 2021;71(6):633–636.
38. Acién P, Bataller A, Fernández F, Acién MI, Rodríguez JM, Mayol MJ. New cases of accessory and cavitated uterine masses (ACUM): a significant cause of severe dysmenorrhea and recurrent pelvic pain in young women. Hum Reprod 2012;27(3):683–694.
39. Ntafam CN, Sanusi-Musa I, Harris RD. Intramural ectopic pregnancy: An individual patient data systematic review. Eur J Obstet Gynecol Reprod Biol X 2023;21:100272.
40. Takeuchi M, Matsuzaki K, Bando Y, Harada M. MR Imaging Findings of Uterine Adenomatoid Tumors. Magn Reson Med Sci 2024;23(2):127–135.
41. Kim JY, Jung KJ, Sung NK, Chung DS, Kim OD, Park S. Cystic adenomatoid tumor of the uterus. AJR Am J Roentgenol 2002;179(4):1068–1070.
42. Giorgi M, Labanca L, Centini G, et al. Extrauterine adenomyoma: A case report and systematic review of the literature. Int J Gynaecol Obstet 2024;164(3):869–901.
43. Batt RE, Smith RA, Buck Louis GM, et al. Müllerianosis. Histol Histopathol 2007;22(10):1161–1166.
44. Batt RE, Yeh J. Müllerianosis: four developmental (embryonic) müllerian diseases. Reprod Sci 2013;20(9):1030–1037.
45. Sajjad N, Iqbal H, Khandwala K, Afzal S. Polypoid Adenomyoma of the Uterus. Cureus 2019;11(2):e4044.
46. Biasioli A, Londero AP, Orsaria M, Scrimin F, Mangino FP, Bertozzi S, et al. Atypical polypoid adenomyoma follow-up and management: Systematic review of case reports and series and meta-analysis. Medicine (Baltimore) 2020;99(26):e20491.
47. Hermens M, van Altena AM, Velthuis I, et al. Endometrial cancer incidence in endometriosis and adenomyosis. Cancers (Basel) 2021;13(18):4592.
48. Moraru L, Mitranovici MI, Chiorean DM, et al. Adenomyosis and Its Possible Malignancy: A Review of the Literature. Diagnostics (Basel) 2023;13(11):1883.
49. Shahnazari R, Shirzadi S, Karaji S, Mokhles P, Far MJG, Maghsudlu S. Endometrial cancer arising from adenomyosis with unusual manifestation: A case report. Clin Case Rep 2023;12(1):e8353.
50. Yuan H, Zhang S. Malignant transformation of adenomyosis: literature review and meta-analysis. Arch Gynecol Obstet 2019;299(1):47–53.
51. Izumi Y, Yamamoto T, Matsunaga N, et al. Endometrial cancer arising from adenomyosis: Case report and literature review of MRI findings. Radiol Case Rep 2020;15(4):427–430.
52. Siegelman ES, Oliver ER. MR imaging of endometriosis: ten imaging pearls. RadioGraphics 2012;32(6):1675–1691.
53. Habiba M, Pluchino N, Petignat P, Bianchi P, Brosens IA, Benagiano G. Adenomyosis and Endometrial Cancer: Literature Review. Vol. 83, Gynecologic and Obstetric Investigation. Gynecol Obstet Invest 2018;83(4):313–328.
54. Furukawa R, Akahane M, Yamada H, et al. Endometrial stromal sarcoma located in the myometrium with a low-intensity rim on T2-weighted images: report of three cases and literature review. J Magn Reson Imaging 2010;31(4):975–979.